Paper

Overcoming Current Quantization Effects for Precise Current Control using Dithering Techniques

Hongzhong Zhu[a)*] Student Member
Hiroshi Fujimoto[*] Senior Member

Accurate current signals are required for precise current control of AC motor drives. However, current measurement errors that involve metering error and quantization error are unavoidable because of the inaccuracy of current sensors and the quantizing feature of analog-to-digital converters in all digital motion control systems. The quantization error contains harmonic components that can induce torque ripple, thus deteriorating the control performance. Therefore, it is necessary to suppress the quantization effects. In this paper, two dithered systems, namely the subtractively dithered system and nonsubtractively dithered system, are presented in order to remove the quantization-based harmonic components of the measured current signals by whitening the quantization error. Moreover, for ease of practical implementation, the design of dither signals is analyzed for nonsubtractively dithered system, considering cases where the metering error is uniform noise or Gaussian noise. It is shown that by applying the dither having a suitably chosen probability density function, the total measurement error can be rendered spectrally white. The effectiveness of the proposed methods is verified through simulations and experiments using a high-precision linear stage.

Keywords: dither, quantization, analog-to-digital converter, current control, AC motor

1. Introduction

Precise current measurement is essential for current control of AC motor drives to achieve high static and dynamic performance [(1)~(3)]. Since the measurement errors are introduced into the control system by current sensors and A/D converters (ADCs), the real current signals of a motor are not guaranteed to follow the reference values exactly. This would induce torque ripple, thus deteriorating the control performance especially when a motion system works at a low load [(4) (5)]. Therefore, understanding and suppressing the effects caused by the current measurement errors have attracted a great deal of attention, see, e.g., [(6)~(9)].

Fig. 1 shows a typical path of the current measurement for current control. Current signals, measured by current sensors, are converted into digital signals via A/D converters after the amplitude amplification and the noise filtering. In this process, the measurement errors that involve metering error and quantization error are introduced into the current control system. Fig. 2 shows the block diagram of the measurement process. The metering error, denoted by η, is mainly caused by the inaccuracy of current sensors and the thermal drift of analog devices in the measurement system. The quantization error, denoted by q, arises because the analog current signal may assume to be any value within the input range of the A/D converters while the output data are finite precision samples. Quantization error behaves as a sort of highly colored noise and cannot be ignored in many cases. It is reported that the quantization error would affect the accuracy of the rotor position estimation when high frequency signal injection method is used for sensorless control [(7)]. In order to reduce quantization effects, the simplest way is to use high-resolution A/D converters, such as sigma-delta A/D converters. However, this would not only increase the implementation cost, but the quantization error cannot be removed completely as well. Moreover, the bandwidth of A/D converter may be limited if a high-resolution one is used, since there is trade-off between the qualitative bandwidth and the resolution of A/D converters.

It is well-known that white noise is easier to be reduced than other colored noise for it contains equal power

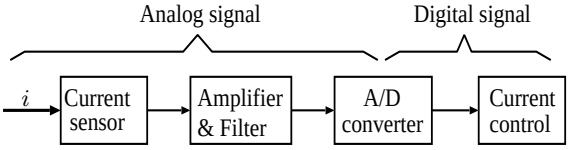

Fig. 1. Path of current measurement.

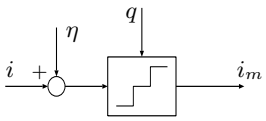

Fig. 2. Block diagram of current measurement: η is the metering noise, and q is the quantization error.

* Department of Electrical Engineering, The University of Tokyo
5-1-5, Kashiwanoha, Kashiwa, Chiba, 277–8561, Japan
a) correspondence to: Hongzhong Zhu. E-mail: zhu@hflab.k.u-tokyo.ac.jp

within a fixed bandwidth at any center frequency. Many methods, such as Kalman filter and LQG controller design methods, are powerful to obtain high control performance if the noise introduced into a system can be treated as white noise [10] [11]. Motivated by this perspective, whitening the quantization error using dithering techniques is considered in this paper. Both the subtractively dithered system and the nonsubtractively dithered system are presented and analyzed. In addition, for ease of practical implementation, the design of dither signals is analyzed for nonsubtractively dithered system, considering cases where η is uniform noise or Gaussian noise.

The remainder of this paper is organized as follows. Section 2 presents some important theorems referring to the quantization and dither. The dithering techniques for suppressing current quantization effects are presented in Section 3. Sections 4 and 5 demonstrate the effectiveness of the proposed approaches via simulations and experiments. Finally, conclusion is given in Section 6.

2. Preliminaries

2.1 Quantization An ideal A/D converter is a nonlinear device having a staircase-type I/O relation, as shown in Fig. 3. Assuming that the input is always within the measurement range of an A/D converter, the output y can be expressed in terms of the input x as

$$y = Q(x) = \Delta \left\lfloor \frac{x}{\Delta} + \frac{1}{2} \right\rfloor, \cdots\cdots\cdots\cdots\cdots\cdots (1)$$

where $Q(\cdot)$ is the quantizing operation, $\lfloor \cdot \rfloor$ denotes the floor operator, and Δ is the quantization step. In the case of current measurement, Δ is given by

$$\Delta = \frac{I_0}{2^{N_b - 1}}, \cdots\cdots\cdots\cdots\cdots\cdots\cdots\cdots\cdots (2)$$

where I_0 is the one-sided measurement range of a current sensor, and $N_b \in \mathbb{N}$ is the resolution of an A/D converter. The quantization error q is defined by

$$q \triangleq Q(x) - x. \cdots\cdots\cdots\cdots\cdots\cdots\cdots\cdots\cdots (3)$$

Generally, q is dependent of x unless x satisfies the so-called band-limited condition, which is also referred to as the "Quantization Theorem" [12]. Although the quantization error q is usually highly colored, its classical model treats it as the uniform noise whose probability density function (pdf) is [13]

$$p_q(\epsilon) = \begin{cases} \frac{1}{\Delta}, & -\frac{\Delta}{2} < \epsilon \leq \frac{\Delta}{2} \\ 0, & \text{otherwise.} \end{cases} \cdots\cdots\cdots\cdots (4)$$

Based on this treatment, the mean and the variance of the quantization error are expressed as

$$E[q] = 0, \cdots\cdots\cdots\cdots\cdots\cdots\cdots\cdots\cdots\cdots (5)$$

$$E[q^2] = \frac{\Delta^2}{12}, \cdots\cdots\cdots\cdots\cdots\cdots\cdots\cdots\cdots (6)$$

where $E[\cdot]$ means the expectation. This treatment is valid for complex input signals whose amplitudes are much larger than the quantization step Δ. However, it fails catastrophically for small or simple signals.

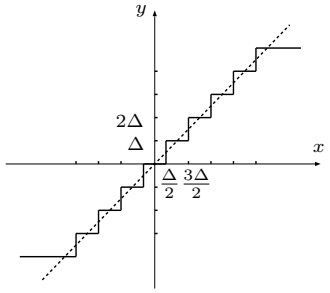

Fig. 3. Quantization characteristic. Δ is the quantization step.

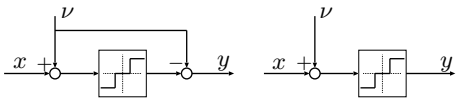

Fig. 4. Dithering systems, x is the input and y is the output, ν denotes the dither. (a): Subtractively dithered system; (b): Nonsubtractively dithered system.

2.2 Dither Dither is an intentionally applied form of noise used to decorrelate signal-dependent noise, and it has been extensively applied to suppress the quantization effects on audio or video signal processing [13] [14]. There exist two archetypes of dithering systems: the subtractively dithered system where the dither is subsequently subtracted from the output signal after quantization, and the nonsubtractively dithered system where the dither is not subtracted from the output signal. Their schematics are shown in Fig. 4. In the case of subtractively dithered system, the total error between the output y and the input x is expressed by

$$\begin{aligned} e &= y - x \\ &= Q(x + \nu) - (x + \nu) \\ &= q(x + \nu), \end{aligned} \cdots\cdots\cdots\cdots\cdots\cdots\cdots\cdots\cdots (7)$$

where ν denotes the dither. It can be shown that [14]:

Schuchman's Condition. In a subtractively dithered system, the total error e is uniformly distributed and statistically independent of the input for arbitrary input distributions if and only if the characteristic function of the dither, denoted by P_ν, satisfies the condition that

$$P_\nu(u)|_{u=k/\Delta} = 0, \quad \text{for } k = \pm 1,\ \pm 2,\ \pm 3, \cdots . \quad (8)$$

Here, the characteristic function of a random variable z is the Fourier transform of its probability density function $p_z(\epsilon)$, which is defined by

$$P_z(u) \triangleq \int_{-\infty}^{\infty} p_z(\epsilon) e^{-j2\pi u\epsilon} d\epsilon. \cdots\cdots\cdots\cdots\cdots\cdots (9)$$

Note that a dither with the uniform probability density function

$$p_\nu(\epsilon) = \begin{cases} \frac{1}{\Delta}, & -\frac{\Delta}{2} < \epsilon \leq \frac{\Delta}{2} \\ 0, & \text{otherwise,} \end{cases} \cdots\cdots\cdots\cdots\cdots (10)$$

has the corresponding characteristic function

$$P_\nu(u) = \frac{\sin(\pi\Delta u)}{\pi\Delta u}, \cdots\cdots\cdots\cdots\cdots\cdots (11)$$

that satisfies the desired condition (8). In this case, the total error e can be rendered to be independent of the input x. In addition, the mean and the variance of the total error e are the same as (5) and (6) [14], which implies that the spectrum level of noise is not enlarged even after introducing an additional noise ν.

The subtractively dithered systems are clearly ideal in the sense that e can be rendered to be independent of the input. The requirement of synchronous dither subtraction at the system output, however, cannot always be implementable in practical situations. For such reason, the nonsubtractively dither technique is also of interest.

In the case of nonsubtractively dithered system, the total error is expressed by

$$\begin{aligned} e &= y - x \\ &= Q(x+\nu) - x \\ &= q(x+\nu) + \nu. \end{aligned} \cdots\cdots\cdots\cdots\cdots\cdots (12)$$

The error e is not simply the quantization error alone, but also involves the dither. Unlike subtractively dithered method, it is proved that the nonsubtractively dithered method cannot render the total error to be statistical independent of the system input, but the following result is obtained [15]:

Theorem. In a nonsubtractively dithered system, $E[e^m]$ is independent of the distribution of the input x if and only if

$$P_\nu^{(m)}(u)\,\big|_{u=k/\Delta} = 0 \quad \text{for } k = \pm 1, \pm 2, \pm 3, \cdots, \quad (13)$$

where $P_\nu^{(m)}(u)$ denotes the m^{th} derivative of $P_\nu(u)$.

It is analyzed in [15] that a dither having a triangular probability density function (triangular-pdf)

$$p_\nu(\epsilon) = \begin{cases} \frac{1}{\Delta^2}(\epsilon + \Delta), & -\Delta < \epsilon \le 0 \\ \frac{1}{\Delta^2}(-\epsilon + \Delta), & 0 < \epsilon \le \Delta \\ 0, & \text{otherwise,} \end{cases} \quad \cdots\cdots (14)$$

whose characteristic function is

$$P_\nu(u) = \left(\frac{\sin(\pi\Delta u)}{\pi\Delta u}\right)^2, \cdots\cdots\cdots\cdots\cdots (15)$$

is a unique choice to render $E[e]$ and $E[e^2]$ to be independent of the input x, while minimizing $E[e^2]$. In this case, the mean and variance of ν and e are expressed by

$$E[\nu] = 0 \cdots\cdots\cdots\cdots\cdots\cdots\cdots\cdots\cdots\cdots (16)$$

$$E[\nu^2] = \frac{\Delta^2}{6} \cdots\cdots\cdots\cdots\cdots\cdots\cdots\cdots\cdots\cdots (17)$$

$$E[e] = 0, \cdots\cdots\cdots\cdots\cdots\cdots\cdots\cdots\cdots\cdots (18)$$

$$E[e^2] = \frac{\Delta^2}{4}. \cdots\cdots\cdots\cdots\cdots\cdots\cdots\cdots\cdots\cdots (19)$$

Therefore, the total error e can also be regarded as white noise for the mean is zero and the variance is a constant value.

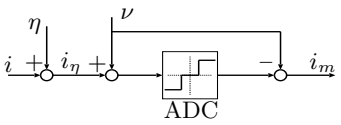

Fig. 5. Model of subtractively dithered method for current quantization.

3. Dithering techniques for current quantization

In this section, dithering techniques introduced in Section 2 are presented to whiten the current quantization error. Both the subtractively dithered approach and the nonsubtractively dithered approach are analyzed. In addition, for ease of practical implementation, the design of dither signals is analyzed for nonsubtractively dithered system, considering cases where η is uniform noise or Gaussian noise.

3.1 Subtractively dithered system The traditional subtractively dithered method is exploited for whitening the current quantization error since it would not enlarge the spectrum level of the total measurement error. The application is shown in Fig. 5. The current error is expressed by

$$\begin{aligned} e_i &= i_m - i \\ &= Q(i_\eta + \nu) - (i_\eta + \nu) + \eta \\ &= q(i_\eta + \nu) + \eta. \end{aligned} \cdots\cdots\cdots\cdots\cdots\cdots (20)$$

According to Schuchman's Condition, $q(i_\eta + \nu)$ is independent of i_η when ν is designed as the uniform noise having the same probability density function as (10). Assuming the metering noise η is white noise and independent and identically distributed (IID) with i and ν, the total current measurement error e_i can be regarded as white noise. The mean and the variance are expressed as

$$E[e_i] = 0, \cdots\cdots\cdots\cdots\cdots\cdots\cdots\cdots\cdots\cdots (21)$$

$$E[e_i^2] = E[\eta^2] + \frac{\Delta^2}{12}. \cdots\cdots\cdots\cdots\cdots\cdots\cdots\cdots\cdots\cdots (22)$$

3.2 Nonsubtractively dithered system The application of nonsubtractively dithered system is shown in Fig. 6. If the traditional nonsubtractively dithered method, namely, designing a dither ν to satisfy the distribution (14), is applied to whiten the quantization error, the variance of the total error e_i is

$$E[e_i^2] = E[\eta^2] + \frac{\Delta^2}{4}, \cdots\cdots\cdots\cdots\cdots\cdots\cdots\cdots\cdots\cdots (23)$$

which may be too large to be acceptable. Therefore, we consider to design ν by taking advantage of the statistical properties of the metering noise η so that the variance of the total error e_i can be decreased. For the sake of convenience, we denote the sum of the dither ν and the metering noise η by

$$w \triangleq \eta + \nu. \cdots\cdots\cdots\cdots\cdots\cdots\cdots\cdots\cdots\cdots\cdots (24)$$

According to the Theorem in Section 2, the optimal choice of ν is the one that can make w have a probability density function equal to the triangular-pdf (14).

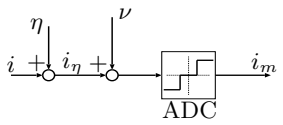

Fig. 6. Model of nonsubtractively dithered method for current quantization.

Assuming that η is zero-mean and has a variance less than $\frac{\Delta}{4}$, a theoretical selection of ν is

$$p_\nu = \mathcal{F}^{-1}\frac{\mathrm{sinc}^2(\pi\Delta u)}{P_\eta(u)}du, \cdots\cdots\cdots\cdots\cdots\cdots (25)$$

where $\mathcal{F}^{-1}$ denotes the inverse Fourier transform, $\mathrm{sinc}(x) = \frac{\sin(x)}{x}$ is known as Sinc function. In (25), $\mathrm{sinc}^2(\pi\Delta u)$ is the characteristic function of triangular-pdf (14) and P_η is the characteristic function of p_η. The formula can be proved according to the convolution theorem. In other words, w can be made to have a probability distribution equal to the triangular-pdf (14) when a dither having a probability density function equal to (25) is applied. In this way, the variance of the total error becomes

$$E[e_i^2] = \frac{\Delta^2}{4}. \cdots\cdots\cdots\cdots\cdots\cdots\cdots\cdots\cdots (26)$$

This value is preferred since it is smaller than (23) and independent of η. However, designing a dither ν to satisfy (25) is usually hard to be realized. According to the practical situations, two common cases that η is uniform noise and η is Gaussian noise are discussed in the following subsection.

3.2.1 The metering error is uniform noise

In order to whiten the quantization error, it is required that w has a probability distribution equal to (14). The following result can be obtained:

Proposition 1. Suppose that η is uniform noise having the probability density function

$$p_\eta(\epsilon) = \begin{cases} \frac{N}{\Delta}, & -\frac{\Delta}{2N} \le \epsilon \le \frac{\Delta}{2N} \\ 0, & \text{otherwise}, \end{cases} \cdots\cdots\cdots\cdots (27)$$

where $N \in \mathbb{N}$ is a natural number, then w has the same probability density function as (14) if the probability density function of ν satisfies

$$p_\nu(\epsilon) = \begin{cases} \frac{1}{N\Delta}, & \begin{cases} -\frac{2N-1}{2N}\Delta < \epsilon \le -\frac{2N-3}{2N}\Delta \\ \frac{2N-3}{2N}\Delta < \epsilon \le \frac{2N-1}{2N}\Delta \end{cases} \\ \frac{2}{N\Delta}, & \begin{cases} -\frac{2N-3}{2N}\Delta < \epsilon \le -\frac{2N-5}{2N}\Delta \\ \frac{2N-5}{2N}\Delta < \epsilon \le \frac{2N-3}{2N}\Delta \end{cases} \\ \vdots & \vdots \\ \frac{i}{N\Delta}, & \begin{cases} -\frac{2(N-i)+1}{2N}\Delta < \epsilon \le -\frac{2(N-i)-1}{2N}\Delta \\ \frac{2(N-i)-1}{2N}\Delta < \epsilon \le \frac{2(N-i)+1}{2N}\Delta \end{cases} \\ \vdots & \vdots \\ \frac{N-1}{N\Delta}, & \begin{cases} -\frac{3}{2N}\Delta < \epsilon \le -\frac{1}{2N}\Delta \\ \frac{1}{2N}\Delta < \epsilon \le \frac{3}{2N}\Delta \end{cases} \\ \frac{1}{\Delta}, & -\frac{1}{2N}\Delta < \epsilon \le \frac{1}{2N}\Delta \\ 0, & \text{otherwise}, \end{cases}$$

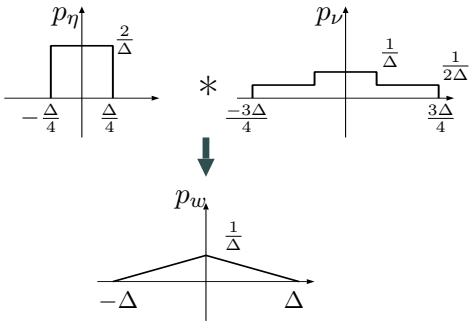

Fig. 7. Example of Proposition 1 in the case of $N = 2$. '$*$' denotes the convolution.

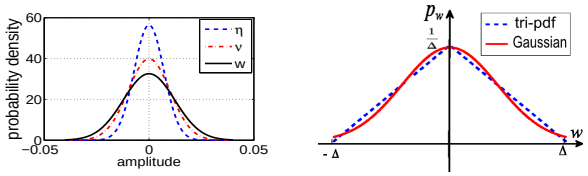

(a) (b)

Fig. 8. (a): Example of $w = \eta + \nu$ from the viewpoint of probability density when η and ν are Gaussian. (b): The comparison of triangular-pdf and Gaussian distribution with the same variance.

$$\cdots\cdots\cdots\cdots\cdots\cdots\cdots\cdots\cdots\cdots (28)$$

where $i = 1, 2, \cdots, N-1$.

□

According to the convolution theorem, the proposition can be proved. Fig. 7 shows an example for calculating p_w from p_η and p_ν in the case of $N = 2$.

If the condition (27) is not satisfied, and η is uniform in $\left[-\frac{\Delta}{2(N+\alpha)} \quad \frac{\Delta}{2(N+\alpha)}\right]$, where $-0.5 < \alpha \le 0.5$, ν can also be designed via (28) by approximating the probability distribution of η to fit the condition (27).

3.2.2 The metering error is Gaussian noise

In many practical situations, sensor noise can be regarded as Gaussian noise. In this case, designing ν based on (25) is not always available not only because of the calculation, but also the implementation. However, according to the convolution theorem and the properties of Normal distribution, the following results can be obtained:

Proposition 2. Suppose that the metering noise η is Gaussian noise and has the Normal distribution:

$$p_\eta(\epsilon) = \frac{1}{\sqrt{2\pi\sigma^2}}e^{-\frac{1}{2}\frac{\epsilon^2}{\sigma^2}}, \quad 0 < \sigma^2 < \frac{\Delta^2}{6}, \cdots\cdots (29)$$

where σ is the standard deviation of η, then w is also Gaussian and has the same variance as (17) if the distribution of ν satisfies

$$p_\nu(\epsilon) = \frac{1}{\sqrt{2\pi(\frac{\Delta^2}{6} - \sigma^2)}}e^{-\frac{1}{2}\frac{\epsilon^2}{\frac{\Delta^2}{6}-\sigma^2}} \cdots\cdots\cdots (30)$$

□

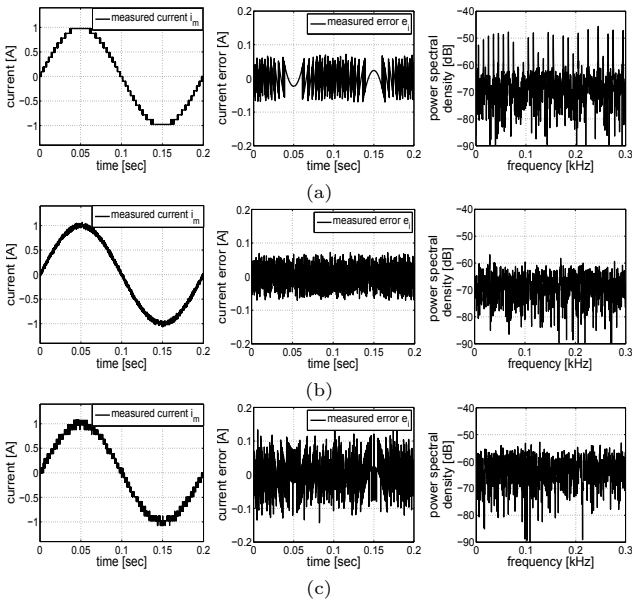

Fig. 9. Simulation results when η is uniform in $[-\frac{\Delta}{4}\ \frac{\Delta}{4}]$. (a) shows the results without applying dither (conventional method). (b) shows the results when subtractive dither is applied. (c) shows the results when nonsubtractive dither designed by (28) is applied. All the left graphs show the measured current i_m, middle graphs show the measurement error e_i, and right graphs show the power spectral density of e_i.

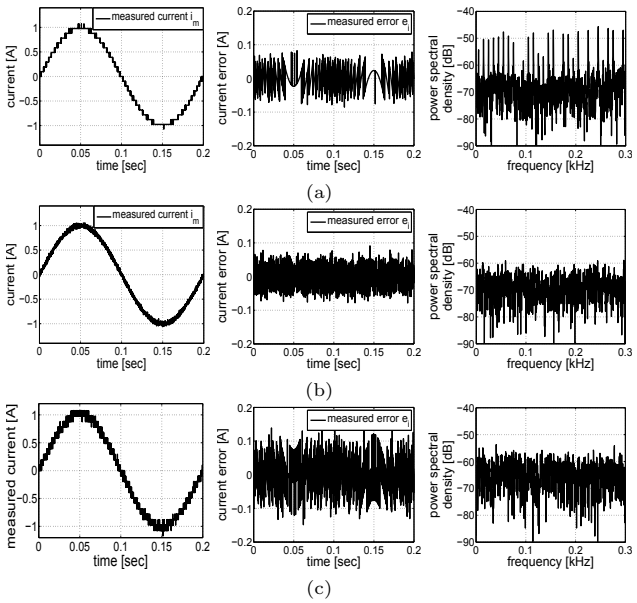

Fig. 10. Simulation results when η is Gaussian. (a) shows the results without applying dither (conventional method). (b) shows the results when subtractive dither is applied. (c) shows the results when nonsubtractive dither designed by (30) is applied. All the left graphs show the measured current i_m, middle graphs show the measurement error e_i, and right graphs show the power spectral density of e_i.

The proposition can be proved according to the Additive Property of Normal distribution. If $\sigma^2 \geq \frac{\Delta^2}{6}$, it can be regarded as that η is large enough to whiten the quantization noise and the dither ν is not necessary. Fig. 8(a) illustrates an example of the sum of two variables from the view of probability density.

It can also be calculated that about 98.5% of values of w are within $[-\Delta\ \Delta]$ (about 2.45-sigma) if ν is designed according to (30). In addition, the difference between Normal distribution and the triangular distribution (14) in $[-\Delta\ \Delta]$ is less than 10%, which is ignorable in many practical situations. Fig. 8(b) shows the comparison of their probability density functions.

4. Simulations

In this section, the simulations are performed to verify the effectiveness of the dithering techniques. An A/D converter with a resolution of 10-bit is supposed to be used. The one-sided measurement range of current sensor is set as $I_0 = 50$A. The corresponding quantization step is $\Delta = 0.0977$ A according to (2). The input current signal is set as sine wave that $i = \sin 10\pi t$ A.

Two situations that η is uniformly distributed in $[-\frac{\Delta}{4}\ \frac{\Delta}{4}]$ and η is Gaussian are examined. In both situations, η is zero-mean and has a variance of $E[\eta^2] = \frac{\Delta^2}{48}$. The following three cases are investigated:

case 1: Without applying dithering techniques;

case 2: With subtractive dither, ν is designed according to (10);

case 3: With nonsubtractive dither considering the statistical characteristics of η, ν is designed according to (28) or (30).

The simulation results are shown in Fig. 9 and Fig. 10. In the figures, (a), (b), and (c) show the results of case 1, case 2, and case 3, respectively. All the left graphs of the figures show the measured current i_m, the middle graphs show the measurement error e_i, and the right graphs show the power spectral density (PSD) of e_i. It is observed from Fig. 9(a) and Fig. 10(a) that the harmonics caused by quantization exist all over the frequency domain. The harmonics are reduced when dithering techniques are applied, which can be observed from Fig. 9(b, c) and Fig. 10(b, c). These results also indicate that the quantization error is whitened. The comparison of the measurement error e_i is shown in Table. 1. The peak value of PSD of e_i and the RMS (root-mean-square), which is defined by

$$e_{\rm rms} := \sqrt{\frac{1}{N}\sum_{j=1}^{N} e_j^2}, \qquad (31)$$

are used for evaluation. Though case 1 can obtain a small RMS of the measurement error, the peak value of PSD is very large, which is not preferred for precise control. Note that the nonsubtractive dithered systems, as analyzed in Section 3, suffered a higher spectrum level of the total measurement error.

5. Experiments

In this section, the effectiveness of the dithering techniques is examined by a high-precision linear stage. Fig. 11 shows the experimental setup. The parameters of

Table 1. Comparison of the measurement error e_i (simulation results)

situations		case 1	case 2	case 3
η is uniform	RMS of e_i ($\times 10^{-4}$)	8.88	9.72	24.3
	$\mathrm{PSD}_{\mathrm{peak}}$ of e_i [dB]	−45.6	−56.9	−52.9
η is Gaussian	RMS of e_i ($\times 10^{-4}$)	9.05	9.79	26.0
	$\mathrm{PSD}_{\mathrm{peak}}$ of e_i [dB]	−45.2	−57.5	−53.1

the stage are shown in Table. 2. The stage is a model of the scanner in exposure system used in the fabrication of the integrated circuits. DSP(TMS320C6713, 225MHz) is used as the processor. U, W-phase current signals are measured by FA-050PV (LEM®) whose measurement range is ±50A. The signals are then converted into digital signals via high-precise A/D converters whose resolution is 14-bit. In order to verify the effectiveness of the dithering techniques, the resolution is dropped to 10-bit by software and the resulting quantization step is $\Delta = 0.0977\,\mathrm{A}$. An accuracy current probe (A662, Tektronix®) is used to measure the real current signal i. Dither is generated in DSP (uniform noise can be generated using the library function "rand()", and Gaussian noise can be generated using "Box-Muller method" [18]) and then converted into analog signals via D/A converters whose resolution is 16-bit. The implementation of dithering techniques is shown in Fig. 12. A time delay is introduced to synchronize the addition and the subtraction when the subtractively dithered method is used. Vector control method with pole-zero cancellation PI current controller is implemented. The block diagram of control system is shown in Fig. 13. A 2-DoF controller which consists of PTC (perfect tracking controller, the feedforward part) and SRC (self resonant cancellation, the feedback part) methods [17] is used to design outer loop controllers to generate current reference.

At first, the statistical property of the metering error is analyzed. The measured current signal converted from high-resolution A/D converter can be regarded as the metering error when control system is at rest. A sample of metering error in time domain is shown in Fig. 14(a). Its histogram plot is shown in Fig. 14(b). It is observed

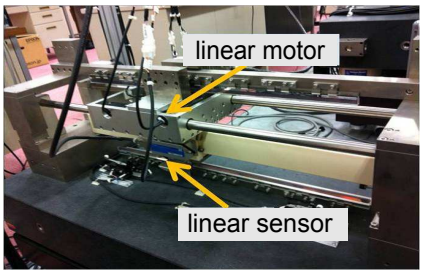

Fig. 11. The experimental setup.

Table 2. Parameters of the stage

Inductance L	15.5×10^{-3}	H
Resistance R	20.5	Ω
Mass M	14.5	kg
Viscosity B	24	N/(m/s)
Thrust coefficient K_t	26.5	N/A
Bach-EMF constant K_e	16	V/(m/s)

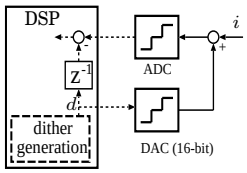

Fig. 12. The implementation of dithering method. The dashed lines show the flow of digital signals, and the solid lines show the flow of analog signals. In order to synchronize the addition and the subtraction, a time delay, denoted by z^{-1}, is introduced.

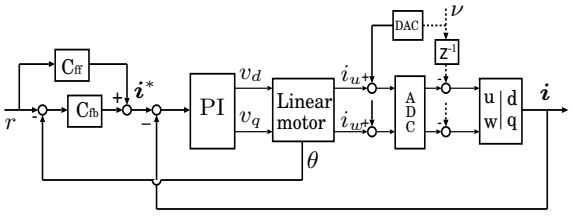

Fig. 13. Block diagram of control system.

that the metering noise can be approximated as Gaussian noise with a variance of $E[\eta^2] = 1.1218 \times 10^{-4}$. Based on this quantity, the nonsubtractively dithered system can be designed according to (30).

In a real scanner system, the exposure is performed during the stage moves at a constant velocity. In order to evaluate the control performance during the exposure, the trajectory reference of the linear stage is set as Fig. 15, and the process that the stage moves at a constant velocity (0.5s∼2.5s) is examined. The experimental results are shown in Fig. 16. In the figure, (a), (b) and (c) show the results of case 1, case 2, and case 3, respectively. The left graphs of Fig. 16(a-c) shows the comparison of the real U-phase current i_u and the measured current i_{u_m}. The right graphs show the PSD of the measurement error e_i. It can be observed from Fig. 16(a) that the harmonics are caused by current quantization error especially at low frequencies. However, these harmonics are suppressed when dithering techniques are applied, which can be observed from the Fig. 16(b, c) that the power spectral density of e_i is flat all over the frequencies. This result indicates that the measurement error is whitened. The RMS of the measurement errors and the peak value of the PSD are summarized in Table. 3. It is observed that though the RMS of the measurement error of case 1 is small, the peak value of the PSD is very large. Fig. 16(d) shows the comparison of force ripple. It can be obtained that the ripple caused by quantization error at high frequencies is suppressed

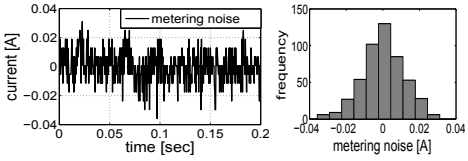

Fig. 14. Example of the metering noise (a) and its histogram analysis (b).

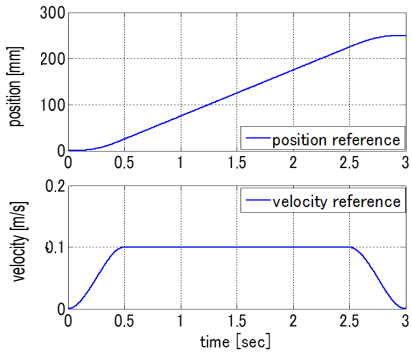

Fig. 15. The position and velocity reference.

Table 3. Comparison of the measurement error (experimental results)

	case 1	case 2	case 3
RMS of e_{i_u} ($\times 10^{-3}$)	1.14	1.07	3.12
$\mathrm{PSD}_{\mathrm{peak}}$ [dB]	−31.8	−42.3	−37.9

Table 4. The RMS of tracking error with & without dither

	case 1	case 2	case 3
tracking error (μm)	3.8118	2.8307	3.0078

by the dithering techniques. The comparison of the position tracking error is shown in Fig. 16(e), and summarized in Table 4. The RMS method defined by (31) is used for evaluation. It is obvious that both subtractively dithered method and nonsubtractively dithered method can obtain better position tracking performance. The subtractive dither method can obtain a relatively small tracking error since it has a lower spectrum level of the total measurement error.

6. Conclusion

In this paper, the dithering methods, namely the subtractively dithered method and the nonsubtractively dithered method, are presented to enhance the current control performance. By applying dithering techniques, the harmonics caused by the current quantization error can be suppressed. Moreover, for ease of practical implementation, the design of dither signals is analyzed for nonsubtractively dithered system, considering cases where the metering error is uniform noise or Gaussian noise. Since the proposed dithering methods have been developed with applicability to actual systems in mind, the implementation is relatively simple. The effectiveness of the dithering techniques is also demonstrated by simulations and experiments. It is obtained that the control performance can be improved when the current quantization error is whitened by dithering techniques.

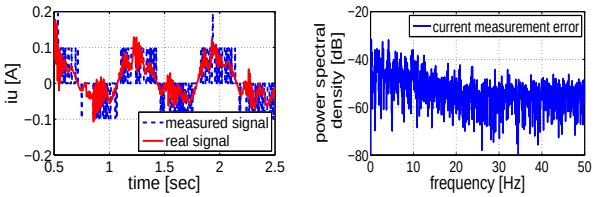

(a) Experimental results without applying dither.

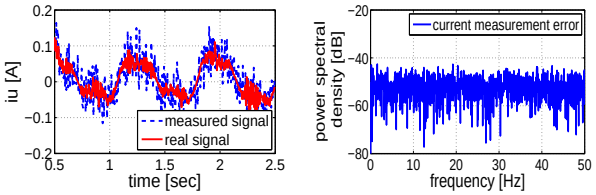

(b) Experimental results with subtractive dither.

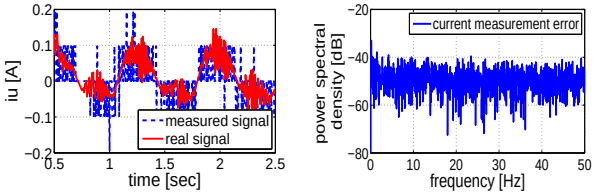

(c) Experimental results with nonsubtractive dither.

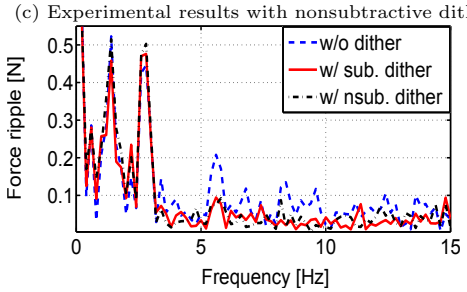

(d) Comparison of the force ripple.

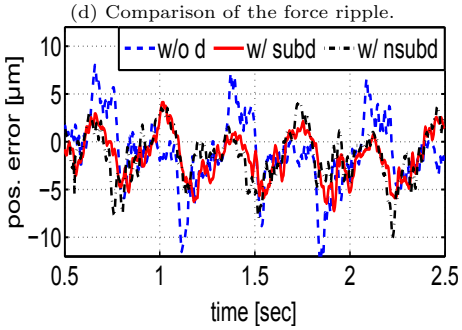

(e) Comparison of position tracking error.

Fig. 16. Experimental results.

References

(1) Mohamed-Wissem Naouar, E. Monmasson, A. A. Naassani, I. S. Belkhodja and N. Patin: "FPGA-Based Current Controllers for AC Machine Drives–A Review", *IEEE Trans. Indust. Electron.*, Vol. 54, No. 4, pp. 1907–1925, Aug. 2007.

(2) J.Rodriguez, J. Pontt, C. A. Silva, P. Correa, P. Lezana, P. Cortes, and U. Ammann: "Predictive Current Control of a Voltage Source Inverter", *IEEE Trans. Indust. appl.* , Vol. 54, No. 1, pp. 495–503, Feb. 2007.

(3) S. Lerdudomsak, S. Doki, and S. Okuma: "Harmonic Currents Estimation and Compensation for Current Control System of PMSM in Overmodulation Range–Analysis for Robustness to Parameter Variations", *IECON*, pp. 1216–1221, Nov. 2008.

(4) J. Holtz, and J. Quan: "Sensorless Vector Control of Induction Motors at Very Low Speed Using a Nonlinear Inverter Model and Parameter Identification", *IEEE Trans. Indust. appl.* , Vol. 38, No. 4, pp. 1087–1095, Jul./Aug. 2002.

(5) K. Nakamura, H. Fujimoto, and M. Fujisuna: "Torque Ripple Suppression Control for PM Motor Considering the Bandwidth of Torque Meter" , *IEEJ Trans. IA* , Vol. 130, No. 11 pp. 1241–1247, 2010 (in Japanese).

(6) D.W. Chung, and S.K. Sul: "Analysis and Compensation of Current Measurement Error in Vector-Controlled AC Motor Drives", *IEEE Trans. Indust. Appl.* , Vol. 34, No. 2, pp. 340–345, Mar./Apr. 1998.

(7) J.H. Jang, S.K. Sul, and Y.C. Son: "Current Measurement Issues in Sensorless Control Algorithm using High Frequency Signal Injection Method", *Proc. IEEE Ind. App. Soc. Annual Meeting* , Vol. 2, pp. 1134–1141, Oct. 2003.
(8) D. Antic, J. B. Klaassens, and W. Deleroi: "Side effects in low-speed AC drives", *Conf. Rec. IEEE-PESC Meeting* , pp. 998–1002, 1994.
(9) C.H. Choi, K.R. Cho, and J.K. Seok: "Inverter Nonlinearity Compensation in the Presence of Current Measurement Errors and Switching Device Parameter Uncertainties", *IEEE Trans. Power Electron.* , Vol.22, No. 2, pp. 576–583, Mar. 2007.
(10) D. Luong-Van, M. Tordon, J. Katupitiya: "Covariance Profiling for an Adaptive Kalman filter to Suppress Sensor Quantization Effects", *Proceedings 43rd IEEE Conference on Decision and Control*, pp. 2680–2685, Dec. 2004.
(11) A. Molin, and S. Hirche: "On LQG Joint Optimal Scheduling and Control under Communication Constraints", *Joint 48th IEEE Conference on Decision and Control and 28th Chinese Control Conference*, pp. 5832–5838, Dec. 2009.
(12) B. Widrow, I. Kollár, and M. Liu: "Statistical Theory of Quantization", *IEEE Trans. Instrum. Meas.*, Vol. 45, No. 2, pp. 353–361, Apr. 1996.
(13) S. P. Lipshitz, R. A. Wannamaker, and J. Vanderkooy: "Quantization and Dither: A Theoretical Survey", *J. Audio Eng. Soc.* , Vol. 40, No.5, pp. 355–375, May 1992.
(14) L. Schuchman: "Dither Signals and Their Effect on Quantization Noise", *IEEE Trans. Commun. Technol.* , pp. 162–165, Dec. 1964.
(15) R. A. Wannamaker, S. P. Lipshitz, J. Vanderkooy, and J. N. Wright: "A Theory of Nonsubtractive Dither", *IEEE Trans. Signal Processing* , Vol. 48, No.2, pp. 499–516, Feb. 2000.
(16) A. B. Sripad, and D. L. Snyder: "A Necessary and Sufficient Condition for Quantization Errors to be Uniform and White", *IEEE Trans. Acoust., Speech, Signal Processing*, Vol. ASSP-25, No. 5, pp. 442–448, Oct. 1977.
(17) K. Sakata, H. Fujimoto: "High Bandwidth Design of Feedback Control System Using Multiple Sensors for High-Precision Stage", *Proc. The 39th SICE Symposium on Control Theory* , pp. 285-290, 2010 (in Japanese).
(18) Mervin E. Muller: "A Comparison of Methods for Generating Normal Deviates on Digital Computers", *Journal of the ACM* , Vol. 6, No. 3, pp. 376–383, Jul. 1959.

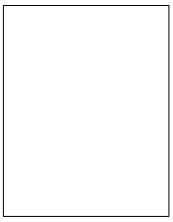

Hongzhong Zhu (Student Member) was born in Fujian, China, on December 27, 1981. He received the MS degree in System Sciences from Kyoto University in 2011, and is presently a Ph.D. student in the Department of Electrical Engineering of The University of Tokyo. His interests are in motion control, convex optimization, and the application of probability theory.

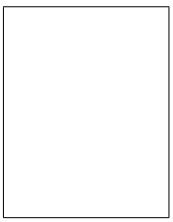

Hiroshi Fujimoto (Senior Member) received the Ph.D. degree in the Department of Electrical Engineering from the University of Tokyo in 2001. In 2001, he joined the Department of Electrical Engineering, Nagaoka University of Technology, Niigata, Japan, as a research associate. From 2002 to 2003, he was a visiting scholar in the School of Mechanical Engineering, Purdue University, U.S.A. In 2004, he joined the Department of Electrical and Computer Engineering, Yokohama National University, Yokohama, Japan, as a lecturer and he became an associate professor in 2005. He is currently an associate professor of the University of Tokyo since 2010. He received the Best Paper Award from the IEEE Transactions on Industrial Electronics in 2001, Isao Takahashi Power Electronics Award in 2010, and Best Author Prize of SICE in 2010. His interests are in control engineering, motion control, nano-scale servo systems, electric vehicle control, and motor drive. Dr. Fujimoto is a member of IEE of Japan, IEEE, the Society of Instrument and Control Engineers, the Robotics Society of Japan, and the Society of Automotive Engineers of Japan.